Nanoscale

PAPER

Electronic Supplementary Information

Reinforcement of Natural Rubber Latex using Lignocellulosic Nanofibers Isolated from Spinifex Grass

Alireza Hosseinmardi[a], Pratheep K. Annamalai[a], Lianzhou Wang[a,b], Darren Martin*[a], Nasim Amiralian*[a]

*Address correspondence to:

n.amiralian@uq.edu.au, darren.martin@uq.edu.au

Introduction

Hemicellulose: Hemicellulose contains branched heterogeneous polymers of pentose (xylose, arabinose), hexose (mannose, glucose, galactose) and acetylated sugars and it is not as chemically homogeneous as cellulose. It has a random, amorphous structure with less strength and hydrolyses easily by dilute acid or base (especially in the case of xylan).[1]

Lignin: Lignin is an amorphous aromatic biopolymer acting as a glue to bind lignocellulose components. It mainly consists of three phenyl propanoid units (p-hydroxyphenyl, guaiacyl and syringyl) which are connected to each other by a series of characteristic linkages (β-O-4, β-5, β-β).[2]

Deep eutectic solvent (DES): In general, the DES is a class of ionic liquid which consists of two components, typically a halide salt of quaternary ammonium or phosphonium cation as a hydrogen bond acceptor (such as choline chloride) and metal chlorides ($ZnCl_2$, $SnCl_2$) or other hydrogen bond donors such as amides, alcohols or acids (such as urea, glycerol) that can all be employed as lignocellulose pretreatments agent.[3-4] Choline chloride and urea at a molar ratio of 1:2 produce a clear homogenous DES with a freezing point of 12 °C. The mixture is a relatively cheap, biodegradable , low toxicity and have a low vapor pressure treatment system.[4-6] Recently, pretreatment of lignocellulose biomass by ionic liquids has gained the intense interest of researchers due to its impressive advantages such as lowering the glass transition temperature (T_g) and plasticizing influence which can increase the flexibility and toughness of these biomaterials.[7-8]

Experimental

XRD analysis was conducted on a Bruker D8 Advance x-ray diffractometer (Bruker, Karlsruhe, Germany) with a Cu Kα source operating at 45 kV and 40 mA. Thermal property of nanocomposite films was evaluated by dynamic mechanical analysis (DMA, SDTABB1[e] Mettler Toledo).

Samples were heated from -90°C to 100°C using the forced vibration method in a tensile mode with a frequency of 1 Hz and a force amplitude of 0.012 N (Displacement amplitude: $\dfrac{50\ \mu m}{9.5\ cm} \times 100 = 0.5\%$).

Results and discussion

Table S1. Influence of CNF variants at different loadings on the initial (zero) shear viscosity (Pa.s) of CNF/NR latex.

CNF content (wt. %) CNF Type	0	0.1	0.5	1	2
NaOH-CNF	0.2	0.1	0.2	0.8	2.3
B-CNF	0.2	0.3	1.5	2.8	4.0
CCU-CNF	0.2	0.2	0.6	1.0	3.1
M-CNF	0.2	0.2	2.3	1.7	27.7

Table S2. Toughness (MJm-3) of different CNF/NR nanocomposites.

CNF content (wt. %) CNF Type	0	0.1	0.5	1	2
NaOH-CNF	125± 14	131± 12	142± 10	114± 7	114± 9
B-CNF	125± 14	127± 3	116 ± 8	91 ± 20	108± 17
CCU-CNF	125± 14	142± 12	127± 12	97 ± 6	94± 6
M-CNF	125± 14	103± 11	97± 15	103 ± 10	75± 16
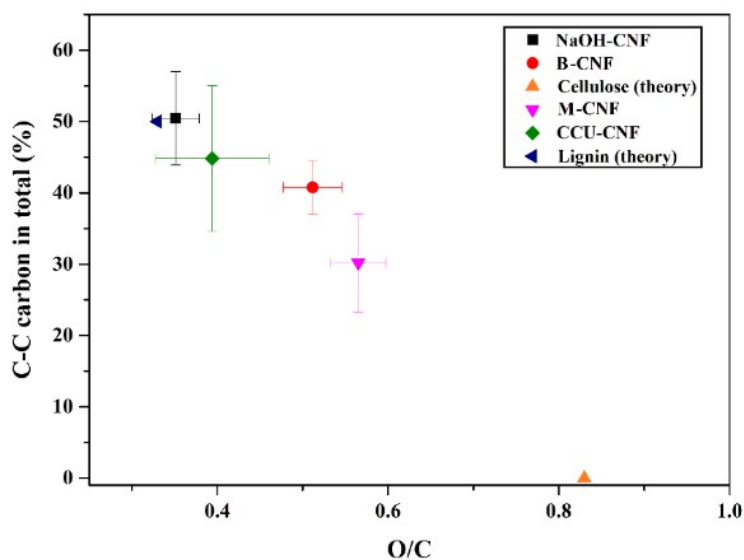
Fig. S1 The percentage of the C-C component as a function of O/C ratio in the CNF variants showing the influence of treatments on the surface functionalities of nanofibers. (An average from scans of five different spots is plotted and compared with the theoretical values for lignin and cellulose).
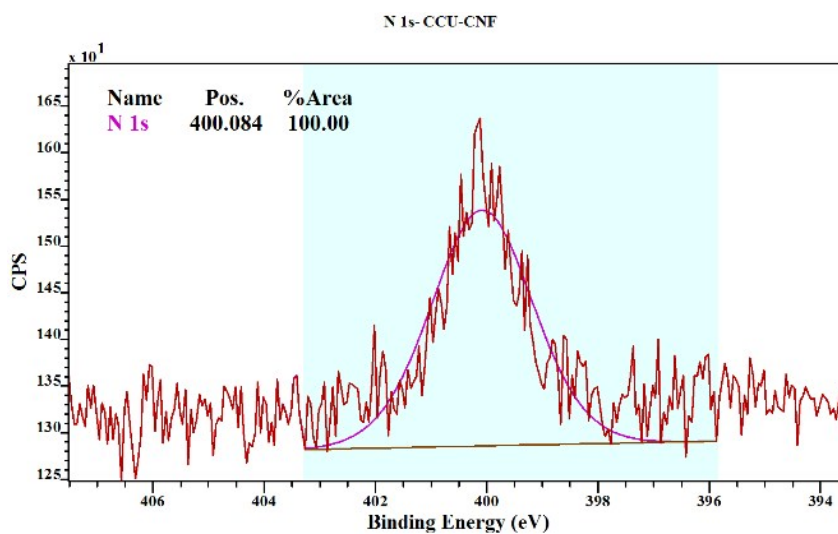
Fig. S2 High-resolution N 1s spectra for CCU-CNF showing the presence of amide bonding.
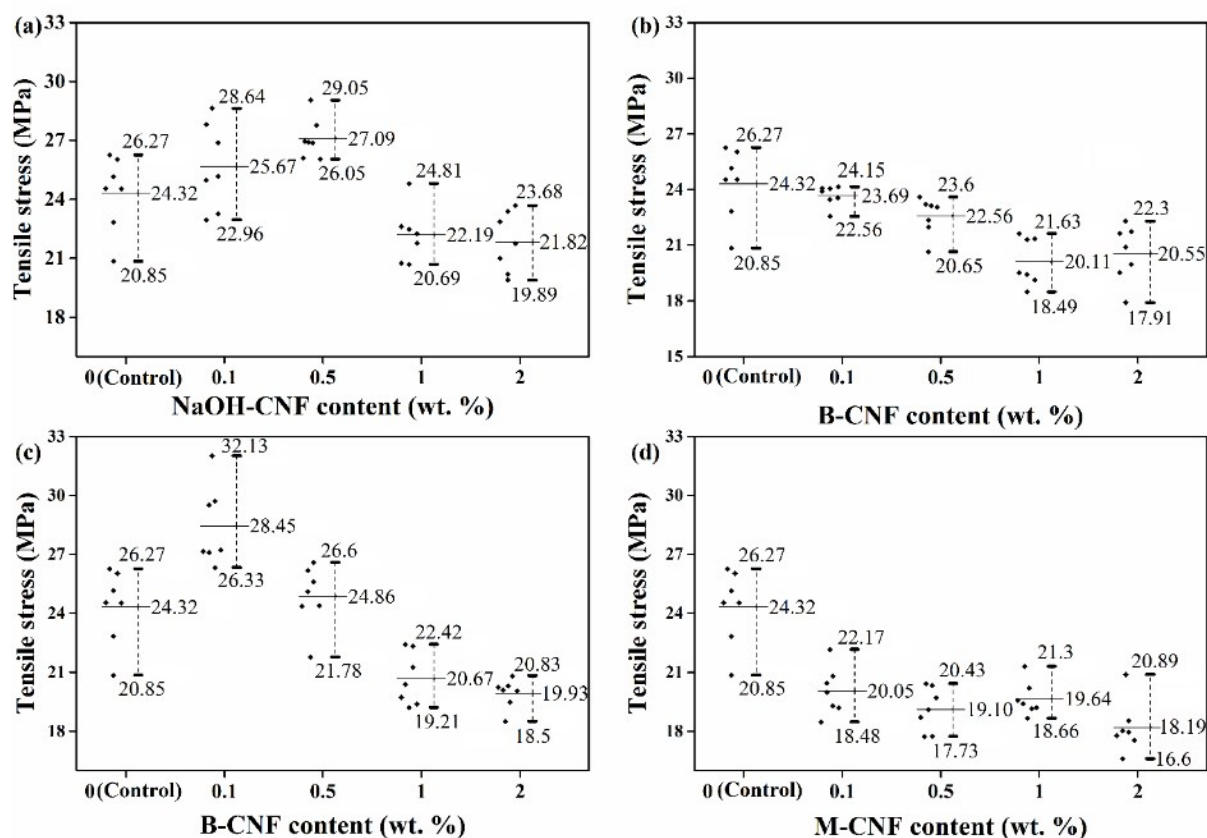
Fig. S3 Tensile stress of NR nanocomposite with (a) NaOH-CNF/NR, (b) B-CNF/NR, (c) CCU-CNF/NR and (d) M-CNF/NR.
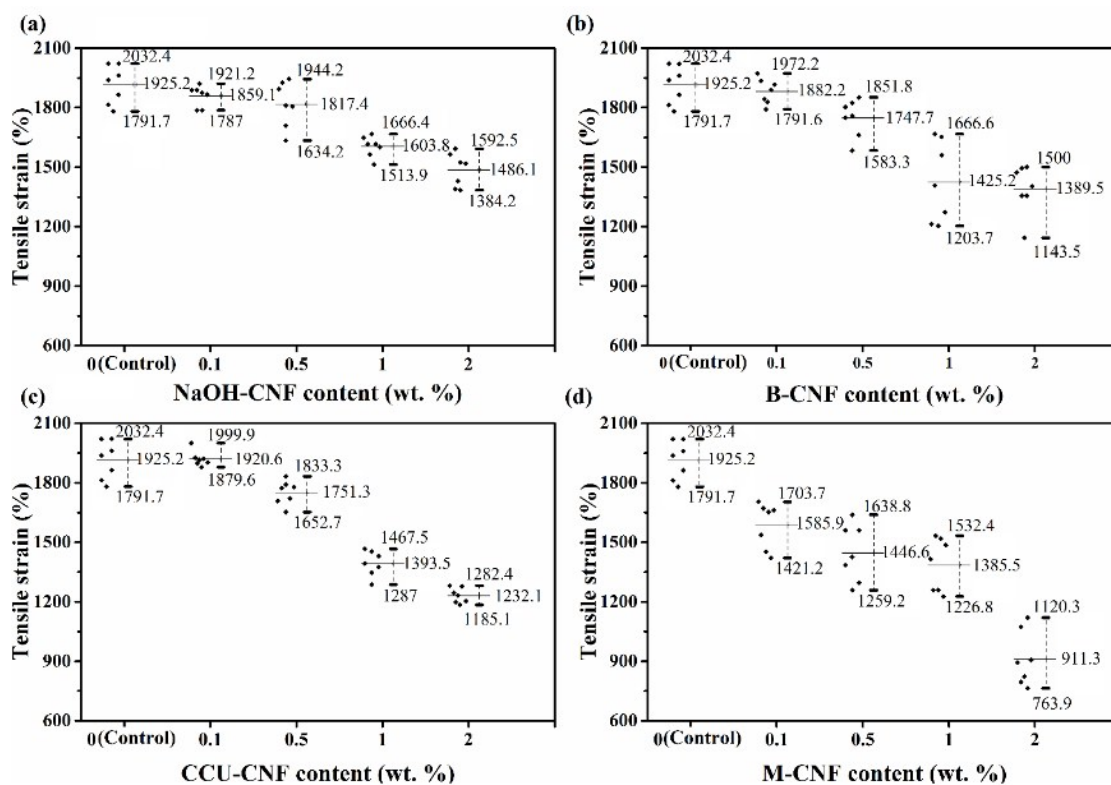
Fig. S4 Tensile strain value of NR nanocomposite with (a) NaOH-CNF/NR, (b) B-CNF/NR, (c) CCU-CNF/NR and (d) M-CNF/NR.
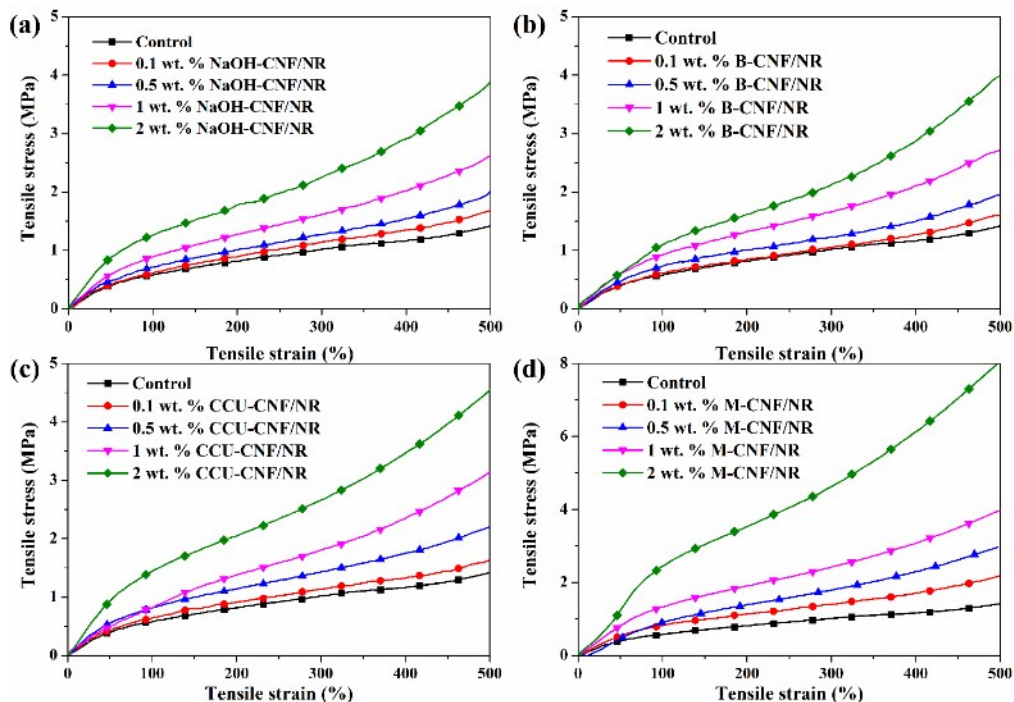
Fig. S5 The stress-strain curve of 500% of NR nanocomposite with (a) NaOH-CNF/NR, (b) B-CNF/NR, (c) CCU-CNF/NR and (d) M-CNF/NR.

DMA analysis: The stiffening effect of nanocomposites with higher loading of various CNF in the NR matrix was investigated using DMA analysis. Fig. S6 shows the evolution of the storage modulus (E') and damping factor (tan δ) as a function of temperature. Storage modulus indicates the effect of fillers stiffening and viscoelastic properties of nanocomposites. The storage modulus of control NR rubber sample shows three different regions: glassy plateau (less than -70 °C), glass transition region (-70 °C to -32 °C) and rubbery plateau (over -32 °C). It can be seen almost the same shape for E' curve by increasing the different type of CNF into the nanocomposites.

The *tan δ* or damping factor (the ratio of energy dissipation as a loss modulus (E") and storage modulus) as a function of temperature corresponds to the amount of energy that can be dissipated in the nanocomposites .[9] The peak of tan δ presents the highest amount of losing energy which indicates the glass transition temperature (T_g). The T_g of the control sample is at -53 °C and by increasing the content of CNF it has not significantly changed. It can be concluded of successfully retaining the stiffness and viscoelastic properties of NR.
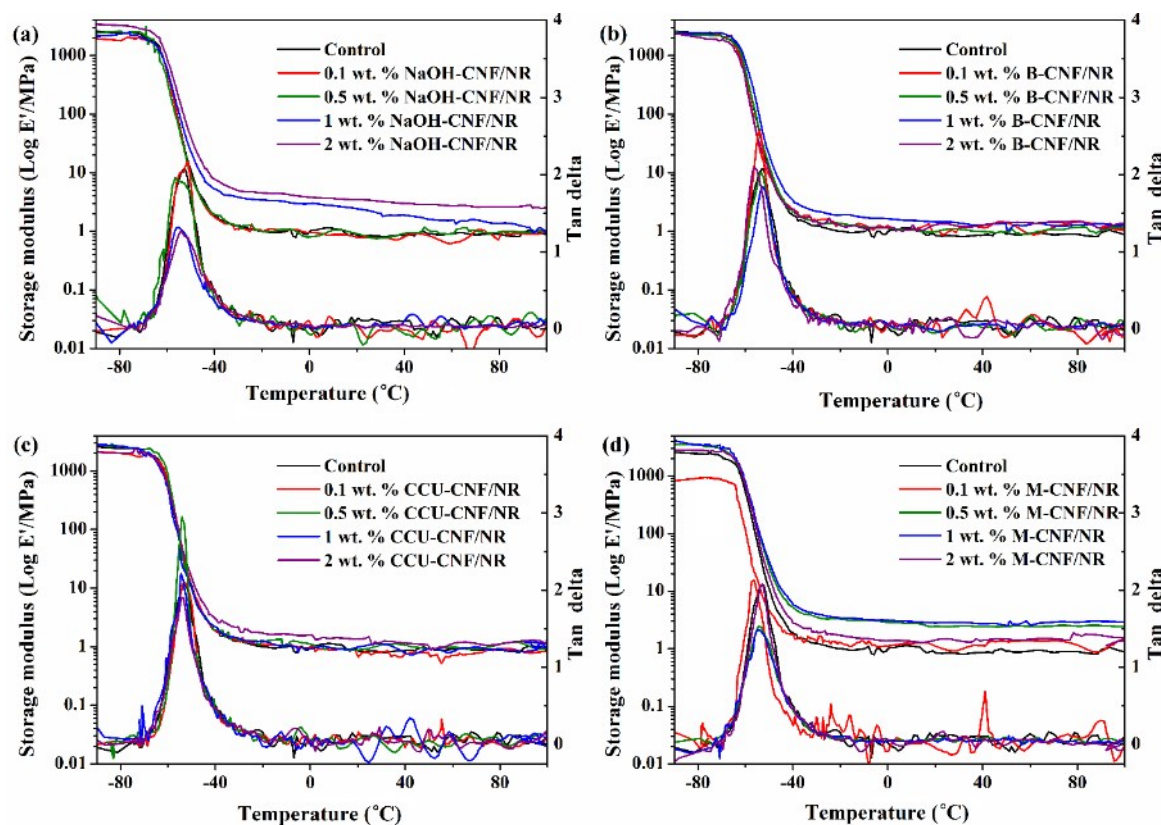
Fig. S6 Storage modules (log E') and *tan δ* curves of (a) NaOH-CNF/NR, (b) B-CNF, (c) CCU-CNF/NR and (d) M-CNF/NR from -90 °C to 100 °C as a function of frequency of 1 Hz. The increasing temperature rate was set at 5 °C/min.

SEM fracture: With increasing the CNF concentration, the nanocomposites showed a very rough fracture surface with ruptured bundles of fibers at the fracture edge after the tensile test (See Fig. S7); due to the poor adhesion between the host matrix and agglomerated nanofillers at higher loading.
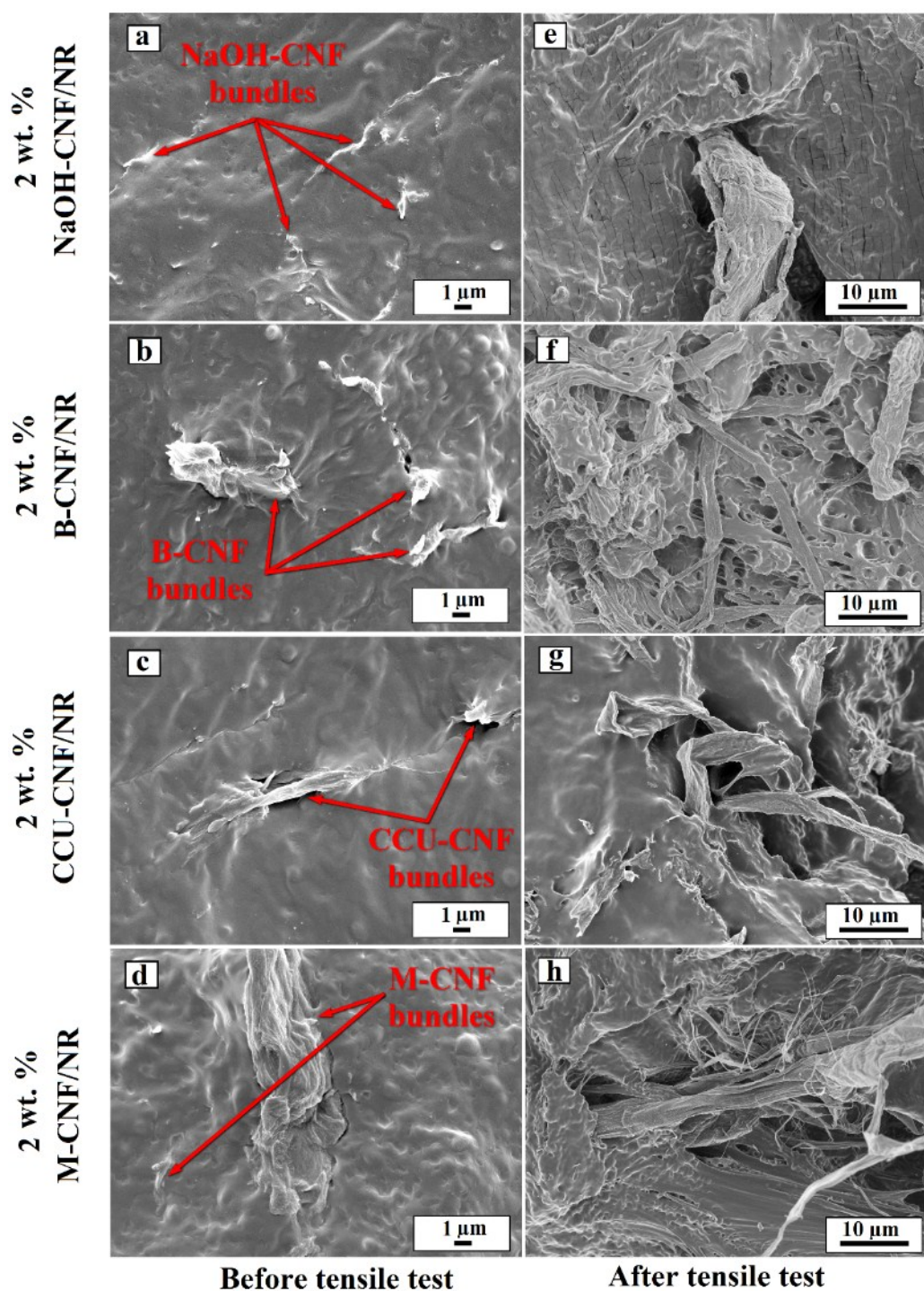
Fig. S7 SEM images of fracture surface of control sample and nanocomposites with 2 wt. % of CNF/NR variants before (left) and after (right) tensile test.

References

1.   Agbor, V. B.; Cicek, N.; Sparling, R.; Berlin, A.; Levin, D. B., Biomass Pretreatment: Fundamentals toward Application. *Biotech. Adv.* **2011,** *29* (6), 675-685.
2.   Jiang, C.; He, H.; Yu, P.; Wang, D. K.; Zhou, L.; Jia, D. M., Plane-Interface-Induced Lignin-based Nanosheets and its Reinforcing Effect on Styrene-Butadiene Rubber. *Express Polym. Lett.* **2014,** *8* (9), 619-634.
3.   Park, J. H.; Oh, K. W.; Choi, H.-M., Preparation and characterization of cotton fabrics with antibacterial properties treated by crosslinkable benzophenone derivative in choline chloride-based deep eutectic solvents. *Cellulose* **2013,** *20* (4), 2101-2114.
4.   Sirvio, J. A.; Visanko, M.; Liimatainen, H., Deep Eutectic Solvent System based on Choline Chloride-Urea as aPre-treatment for Nnanofibrillation of Wood Cellulose. *Green Chem.* **2015,** *17* (6), 3401-3406.
5.   Abbott, A. P.; Capper, G.; Davies, D. L.; Rasheed, R. K.; Tambyrajah, V., Novel Solvent Properties of Choline Chloride/Urea mixtures. *Chem. Commun.* **2003,** (1), 70-71.
6.   Abbott, A. P.; Bell, T. J.; Handa, S.; Stoddart, B., Cationic Functionalisation of Cellulose using a Choline based Ionic Liquid Analogue. *Green Chem.* **2006,** *8* (9), 784-786.
7.   Shamsuri, A. A.; Daik, R., Plasticizing Effect of Choline Chloride/urea Eutectic-based Ionic Liquid on Physicochemical Properties of Agarose Films. *BioResources* **2012,** *7* (4), 4760-4775.
8.   Procentese, A.; Johnson, E.; Orr, V.; Garruto Campanile, A.; Wood, J. A.; Marzocchella, A.; Rehmann, L., Deep Eutectic Solvent Pretreatment and Subsequent Sccharification of Corncob. *Bioresource Tech.* **2015,** *192*, 31-36.
9.   Jabbar, A.; Militký, J.; Wiener, J.; Kale, B. M.; Ali, U.; Rwawiire, S., Nanocellulose Coated Woven jute/Green epoxy Composites: Characterization of Mechanical and Dynamic Mechanical Behavior. *Compos. Struct.* **2017,** *161*, 340-349.